Retrieval and validation of forest background reflectivity from daily MODIS bidirectional reflectance distribution function (BRDF) data across European forests

Jan Pisek[1]*, Angela Erb[2], Lauri Korhonen[3], Tobias Biermann[4], Arnaud Carrara[5], Edoardo Cremonese[6], Matthias Cuntz[7], Silvano Fares[8], Giacomo Gerosa[9], Thomas Grünwald[10], Niklas Hase[11], Michal Heliasz[4], Andreas Ibrom[12], Alexander Knohl[13], Johannes Kobler[14], Bart Kruijt[15], Holger Lange[16], Leena Leppänen[17], Jean-Marc Limousin[18], Francisco Ramon Lopez Serrano[19], Denis Loustau[20], Petr Lukeš[21], Lars Lundin[22], Riccardo Marzuoli[9], Meelis Mölder[4], Leonardo Montagnani[23], Johan Neirynck[24], Matthias Peichl[25], Corinna Rebmann[11], Eva Rubio[19], Margarida Santos-Reis[26], Crystal Schaaf[2], Marius Schmidt[27], Guillaume Simioni[28], Kamel Soudani[29], and Caroline Vincke[30]

[1]Tartu Observatory, University of Tartu, Observatooriumi 1, Tõravere, 61602, Tartumaa, Estonia
[2]University of Massachusetts Boston, Boston, Boston, USA
[3]University of Eastern Finland, Joensuu, Finland
[4]Lund University, Lund, Sweden
[5]Fundacion CEAM, Paterna, Spain
[6]ARPA Valle d'Aosta, Saint Christophe, Italy
[7]Université de Lorraine, AgroParisTech, INRAE, UMR Silva, Nancy, France
[8]CNR-National Research Council, Rome, Italy
[9]Università Cattolica del Sacro Cuore, Brescia, Italy
[10]Technische Universität Dresden, Dresden, Germany
[11]Helmholtz Centre for Environmental Research - UFZ, Leipzig, Germany
[12]Technical University of Denmark, Kongens Lyngby, Denmark
[13]University of Göttingen, Göttingen, Germany
[14]Umweltbundesamt, Vienna, Austria
[15]Wageningen University & Research, Wageningen, Netherlands
[16]Norwegian Institute of Bioeconomy Research, Ås, Norway
[17]Finnish Meteorological Institute, Space and Earth Observation Centre, Sodankylä, Finland
[18]CEFE Univ Montpellier, CNRS, EPHE, IRD, Univ Paul Valéry Montpellier, Montpellier, France
[19]IER-ETSIAM, Universidad de Castilla-La Mancha, Albacete, Spain
[20]INRAe, Bordeaux, France
[21]Global Change Research Institute, Academy of Sciences of the Czech Republic, Brno, Czech Republic
[22]Swedish University of Agricultural Sciences, Uppsala, Sweden
[23]Free University of Bolzano, Bolzano, Italy, and 23b Forest Services, Autonomous Province of Bolzano, Bolzano, Italy
[24]INBO, Geraardsbergen, Belgium
[25]Department of Forest Ecology and Management, Swedish University of Agricultural Sciences, Umeå, Sweden
[26]cE3c – Centre for Ecology, Evolution and Environmental Changes, Lisbon, Portugal
[27]Forschungszentrum Juelich, Juelich, Germany
[28]INRAe - URFM, Avignon, France
[29] Université Paris-Saclay, CNRS, AgroParisTech, Ecologie Systématique et Evolution, 91405, Orsay, France
[30]Université Catholique de Louvain, Louvain-la-Neuve, Belgium

Correspondence to: Jan Pisek (janpisek@gmail.com)

Abstract. Information about forest background reflectance is needed for accurate biophysical parameter retrieval from forest canopies (overstory) with remote sensing. Separating under and overstory signals would enable more accurate modeling of forest carbon and energy fluxes. We retrieved values of normalized difference vegetation index (NDVI) of forest understory with multi-angular Moderate Resolution Imaging Spectroradiometer (MODIS) bidirectional reflectance distribution function (BRDF)/albedo data (gridded 500 meter daily Collection 6 product), using a method originally developed for boreal forests. The forest floor background reflectance estimates from MODIS data were compared with *in situ* understory reflectance measurements carried out at an extensive set of forest ecosystem experimental sites across Europe. The reflectance estimates from MODIS data were hence tested across diverse forest conditions and phenological phases during the growing season, to examine its applicability on ecosystems other than boreal forests. Here we report the method can deliver good retrievals especially over different forest types with open canopies (low foliage cover). The performance of the method was found limited over forests with closed canopies (high foliage cover), where the signal from understory gets much attenuated. The spatial heterogeneity of individual field sites as well as the limitations and documented quality of the MODIS BRDF product are shown to be important for correct assessment and validation of the retrievals obtained with remote sensing.

1 Introduction

The reflectance from the forest canopy background/forest floor can often confound and even dominate the radiometric signal from the upper forest canopy layer to the atmosphere. Forest understory is defined here as all the components found under the forest canopy: understory vegetation, leaf litter, moss, lichen, rock, soil, snow, or a mixture thereof (Pisek and Chen, 2009). If unaccounted for, forest understory can introduce potential bias in the estimation of overstory biophysical parameters (e.g. leaf area index (LAI), fraction of absorbed photosynthetically active radiation (fAPAR)) and, subsequently, productivity estimates (e.g. the net primary productivity (NPP)) as the contribution of the understory to the total energy absorption capacity of a forest stand can be quite significant (Clark et al. 2001; Law et al. 2001). The understory vegetation in forest ecosystems should be treated differently from overstory in carbon cycle modelling because of different residence times of carbon fixed through net primary productivity in different ecosystem components (Vogel and Gower, 1998; Rentsch et al., 2003; Marques and Oliveira, 2004; Kim et al., 2016). Currently, the understory is often treated as an unknown quantity in carbon models due to the difficulties in measuring it properly and consistently across larger scales (Luyssaert et al., 2007). The predictions regarding spectral variation of forest background have posed persistent challenge (McDonald et al., 1998; Gemmell, 2000) because of the high variability of incoming radiance below the forest canopy, challenges with the spectral characterization and weak signal in some parts of the spectrum for both overstory and understory (Schaepman et al., 2009), and the general varying nature of the understory (Miller et al., 1997).

Multi-angle remote sensing can capture signals of different forest layers because the observed proportions for different forest layers vary with the viewing angle, making it possible to separate forest overstory and understory signal. Here, we aim at consolidating previous efforts of tracking understory reflectance and its dynamics with multi-angle Earth observation data

(Canisius and Chen, 2007; Pisek and Chen, 2009; Pisek et al., 2010, 2012, 2015a, 2015b, 2016; Jiao et al., 2014) by testing the validity of this approach using Moderate Resolution Imaging Spectroradiometer bidirectional reflectance distribution function (MODIS BRDF)/albedo data (gridded 500 meter daily Collection 6 MCD43 product) against *in situ* understory reflectance measurements over an extended set of Integrated Carbon Observation System (ICOS) forest ecosystem sites. The validation procedure was defined to comply as much as possible with the best practices proposed by the Committee on Earth Observation Satellites (CEOS) Working Group on Calibration and Validation (WGCV) Land Product Validation (LPV) subgroup (Garrigues et al., 2008; Baret et al., 2006). It corresponds to Stage 1 validation as defined by the CEOS (Nightingale et al., 2011; Weiss et al., 2014), where product accuracy shall be assessed over a small (typically < 30) set of locations and time periods by comparison with *in situ* or other suitable reference data. Using the extended set of ICOS forest ecosystems as validation sites, we asked the following questions:

1. Can ICOS forest ecosystem sites serve as a suitable validation dataset with respect to their footprint and the pixel resolution of EO products?

2. Can we retrieve reliable normalized difference vegetation index (NDVI; Rouse et al., 1973; Tucker, 1979) dynamics for understory with MODIS BRDF data across diverse forest conditions during the growing season?

3. Are there important differences between the total (overstory+understory) and understory-only NDVI signal?

2 Materials and Methods

2.1 Study sites

The Integrated Carbon Observation System (ICOS) is a distributed pan-European research infrastructure providing *in situ* standardized, integrated, long-term and high-precision observations of lower atmosphere greenhouse gas (GHG) concentrations and land- and ocean-atmosphere GHG interactions (Gielen et al., 2017). In this study we carried out the evaluation over the network of 31 ICOS-affiliated forest ecosystem sites, complemented with additional sites in Spain, Portugal, Austria, and Finland. Together these selected 40 study sites comprise a large variety of forest over- and understory types, spanning a wide latitudinal gradient from almost 38°N (Yeste, Spain) to 68°N (Kenttärova, Finland). Site locations are shown in Figure 1 and vegetation characteristics are summarized in Table 1.

2.2 Understory spectra and forest canopy cover/closure in situ measurements

Following the terminology by Schaepman-Strub et al. (2006), we refer to the reflectance factors measured by the field spectrometers as to the satellite derived hemispherical-directional reflectance factors (HDRFs). The given spectrometer's field of view is approximated as angular (cone) and narrower than a whole hemisphere, with some anisotropy captured which corresponds to normal remote sensing viewing geometry. An overview of the undertaken *in situ* campaigns at each site as well as their characteristics is given in Table 1.

110

Figure 1. Distribution of study sites across Europe; for further details, refer to Table 1.

The individual sites were visited between April 2017 and August 2019, mostly during the growing season. Following the protocol by Rautiainen et al. (2011), the understory spectra were measured with sun completely obscured by the clouds, or

115 around sunset (diffuse light conditions) covering the visible/NIR region depending on the spectrometer (see Table 1 for more details). Three understory spectra were measured every 2 m along two 50 m long transects laid at each site, resulting in 50 measurement points (150 individual measurements). Transects covered and characterized conditions within the measurement footprint of the given tower. It should be noted that the tower footprint might be different from the exact MODIS pixel footprint (see section 2.5 for the spatial homogeneity assessment of MODIS pixels). The measurements concerned conditions at the

120 forest floor and low herbaceous and shrubby species or tree seedlings and saplings, as the area sampled by each spectral measurement was estimated to correspond to a ~ 50 cm diameter circle on the ground. The downward-pointed spectroradiometer (no fore-optics were used) was held by the operator's out-stretched hand. Three spectra above a 10-inch Spectralon SRT-99–100 white panel were recorded at the beginning, after every four understory spectra measurement points (every 8 m), and at end of each transect. A hemispherical-conical reflectance factor was obtained with an "uncalibrated"

125 Spectralon reflectance spectrum and the linearly interpolated irradiance. Finally, broadband HDRFs for red (620–670 nm) and NIR (841–876 nm) wavelengths were computed with relative spectral response functions for the MODIS sensor on-board Terra. Understory NDVI value for given site was calculated from the red and NIR band values and averaged over the two transects.

4

Table 1. Study site characteristics and their spatial representativeness status. ICOS - Integrated Carbon Observing System sites; LTER - Long Term Ecological Research Network sites.

Site Code	Site Name	Lat (deg)	Lon (deg)	Sampling date	Spectrometer model	Understory vegetation	Representativeness
AT_Zbn	Zoebelboden (LTER)	47.842	14.442	20171118	ASD FieldSpec 4	Calamagrostis varia, Brachypodium sylvaticum, Hordelymus europaeus, Senecio ovatus	Not Representative
BE-Bra	Brasschaat (ICOS)	51.304	4.519	20190112	Ocean Optics FLAME-S-VIS-NIR-ES	Betula spec, Quercus robur, Sorbus aucuparia	Representative
BE-Vie	Vielsalm (ICOS)	50.3	5.983	20180816	Ocean Optics FLAME-S-VIS-NIR-ES	sparse fern and moss cover	Representative @ 0.5 km
CH-Dav	Davos (ICOS)	46.817	9.85	20180712	Ocean Optics FLAME-S-VIS-NIR-ES	dwarf shrubs, blueberry , mosses	Representative
CZ-BK1	Bílý Kříž (ICOS)	49.502	18.539	20160417	ASD FieldSpec 4	Vaccinium myrtillus L.	Representative @ 1.5 km
CZ-Lnz	Lanžhot (ICOS)	48.682	16.948	20170427	ASD FieldSpec 4	Allium ursinum, Asarum europeum	Representative
DE-Hai	Hainich (ICOS)	51.079	10.453	20180412	Ocean Optics FLAME-S-VIS-NIR-ES	Anemone nemorosa, Allium ursinum	Representative
DE-HoH	Hohes Holz (ICOS)	52.083	11.217	20180411	Ocean Optics FLAME-S-VIS-NIR-ES	Anemone nemorosa	Representative
DE-RuW	Wüstebach (ICOS)	50.505	6.331	20180816	Ocean Optics FLAME-S-VIS-NIR-ES	sparse Deschampsia flexuosa, Deschampsia cespitosa, Molinia caerulea	Not Representative
DE-Tha	Tharandt (ICOS)	50.967	13.567	20180412	Ocean Optics FLAME-S-VIS-NIR-ES	Fagus sylvatica, Abies alba, Deschampsia flexuosa	Representative
DK-Sor	Soroe (ICOS)	55.486	11.645	20180926	Ocean Optics FLAME-S-VIS-NIR-ES	beech saplings and seedlings, Pteridium Aquilinum	Representative
ES-AP1	Almodovar del Pinar	39.677	-1.848	20171109	ASD FieldSpec HandHeld 2	Quercus ilex ssp ballota, Rosmarinus officinalis, Thymus vulgaris, Lavandula latifolia, Quercus coccifera, Genista scorpius	Representative
ES-CMu	Cuenca des Majadas	40.252	-1.965	20171112	ASD FieldSpec HandHeld 2	Juniperus communis, Juniperus oxycedrus, Crataegus monogyna	Representative @ 0.5 km
ES-CPa	Cortes de Pallas	39.224	-0.903	20171108	Ocean Optics FLAME-S-VIS-NIR-ES	Rosmarinus officinalis, Ulex parviflorus, Brachypodium retusum	Representative > 0.5 km
ES-Yst	Yeste	38.339	-2.351	20180728	Ocean Optics FLAME-S-VIS-NIR-ES	Rosmarinus officinalis L., Thymus vulgaris L., Cistus clusii Dunal	Representative @ 0.5 km
FI-Hal	Halssiaapa	67.368	26.654	20170613	ASD FieldSpec Pro	sedge vegetation	Representative
FI-Hyy	Hyytiälä (ICOS)	61.847	24.295	20180628	Ocean Optics FLAME-S-VIS-NIR-ES	Vaccinium spec ., Norway spruce seedlings	Representative @ 0.5 km
FI-Ken	Kenttarova (ICOS)	67.987	24.243	20170613	ASD FieldSpec Pro	Vaccinium myrtillus, Empetrum nigrum, Vaccinium vitis-idaea and the forest mosses Pleurozium schreberi, Hylocomium splendens, Dicranum polysetum	Representative @ 2 km
FI-Kns	Kalevansuo	60.647	24.356	20170615	ASD FieldSpec Pro	dwarf shrubs, mosses	Representative @ 0.275 km
FI-Let	Lettosuo (ICOS)	60.642	23.96	20170615	ASD FieldSpec Pro	dwarf shrubs, mosses, herbs	Representative < 1.0 km
FI-Sod	Sodankylä (ICOS)	67.362	26.638	20170613	ASD FieldSpec Pro	lingonberry, Calluna vulgaris, lichens	Spheroid not fit < 1.5 km;Not represenative at > 1.5 km
FI-Var	Värriö (ICOS)	67.757	29.616	20170614	ASD FieldSpec Pro	mosses, lichens, dwarf shrubs	Representative
FR-Bil	Bilos-Salles (ICOS)	44.494	-0.956	20180614	Ocean Optics FLAME-S-VIS-NIR-ES	Molinia coerulea Moench ., Pteridium aquilineum , Ulex europaeus	Representative < 0.5 km

5

Table 1. (continued)

Site Code	Site Name	Lat (deg)	Lon (deg)	Sampling date	Spectrometer model	Understory vegetation	Representativeness
FR-FBn	Font Blanche (ICOS)	43.241	5.679	20180612	Ocean Optics FLAME-S-VIS-NIR-ES	Quercus coccifera, Phillyrea latifolia, and other species	Representative @ 1.5 km
FR-Fon	Fontainebleau-Barbeau (ICOS)	48.476	2.780	20180616	Ocean Optics FLAME-S-VIS-NIR-ES	Carpinus betulus	Representative @ 0.5 km
FR-Hes	Hesse (ICOS)	48.674	7.066	20180818	Ocean Optics FLAME-S-VIS-NIR-ES	Fagus sylvatica seedlings, blackberry	Spheroid not fit
FR-MsS	Montiers (ICOS)	48.537	5.312	20190114	Ocean Optics FLAME-S-VIS-NIR-ES	sparse Sphagnum spec. Vegetation	Representative > 1.0 km
FR-Pue	Puechabon (ICOS)	43.741	3.596	20180613	Ocean Optics FLAME-S-VIS-NIR-ES	Buxus sempervirens, Pistacia lentiscus, Phillyrea latifolia, Salvia rosmarinus, Ruscus aculeatus	Representative
IT-BFt	Bosco Fontana (ICOS)	45.202	10.743	20180710	Ocean Optics FLAME-S-VIS-NIR-ES	Hedera helix, Corylus spec., Ruscus aculeatus	Representative @ 1.5 km
IT-Cp2	Castelporziano2 (ICOS)	41.704	12.357	20190125	Ocean Optics FLAME-S-VIS-NIR-ES	Phyllirea latifolia, Pistacia lentiscus	Representative @ 1.5 km
IT-Ren	Renon (ICOS)	43.732	10.291	20180711	Ocean Optics FLAME-S-VIS-NIR-ES	Deschampsia flexuosa L. , Vaccinium myrtillus L. , Rhododendron ferrugineum L.	Representative @ 0.5 km
IT-SR2	San Rossore (ICOS)	61.847	24.295	20180628	Ocean Optics FLAME-S-VIS-NIR-ES	Ligustrum vulgare	Representative < 1.5 km
IT-Trf	Torgnon	45.833	7.567	20180707	Ocean Optics FLAME-S-VIS-NIR-ES	Juniperus communis, Rhododendron ferrugineum, Festuca varia	Not Representative
NL-Loo	Loobos (ICOS)	52.167	5.744	20180813	Ocean Optics FLAME-S-VIS-NIR-ES	Prunus serotina, Vaccinium Myrtilus, Deschampsia felexuosa, mosses	Representative @ 0.5 km
NO-Hur	Hurdal (ICOS)	60.372	11.078	20180927	Ocean Optics FLAME-S-VIS-NIR-ES	Vaccinium spec., Norway spruce seedlings	Representative
PT-Cor	Coruche (LTER)	39.138	-8.333	20161008	Ocean Optics FLAME-S-VIS-NIR	Rumex acetosella, Tuberaria guttata, Tolpis barbata Plantago coronopus, Agrostis pourretii, Briza maxima, Vulpia bromoides, V. Geniculata	Spheroid not fit
SE-Htm	Hyltemossa (ICOS)	56.098	13.419	20180928	Ocean Optics FLAME-S-VIS-NIR-ES	continuous moss cover	Spheroid not fit
SE-Knd	Kindla (LTER)	59.754	14.908	20160716	ASD FieldSpec Pro	ericaceous dwarf-shrubs, mosses and lichens	Representative
SE-Nor	Norunda (ICOS)	60.086	17.48	20181022	ASD FieldSpec Pro	bilberry, lingonberry, moss	Representative < 1.5 km
SE-Svb	Svartberget (ICOS)	64.256	19.775	20190823	ASD FieldSpec Pro	bilberry, lingonberry and moss	Representative

Estimates of overstory foliage cover and crown cover were obtained from digital cover photographs (DCP). Overstory foliage cover was defined as the % ground covered by the vertical projection of foliage and branches, and crown cover as the % ground covered by the vertical projections of outermost perimeters of the crowns on the horizontal plane (without double-counting overlap) (Gschwantner et al., 2009). The DCPs were taken from below the canopy every 8 meters along transects at each site. The camera (Nikon CoolPix4500, 2272 x 1704 resolution) was set to automatic exposure, aperture-priority mode, minimum aperture and F2 lens (Macfarlane et al., 2007). The camera was levelled at the height of 1.4 m above the ground and the lens was pointed towards zenith. This setup provides a view zenith angle from 0 to 15 degrees, which is comparable with the 1st ring of the LAI-2000 instrument (Macfarlane et al., 2007).

We used the algorithm by Nobis and Hunziker (2005) to threshold a majority of the DCP images. However, some of the images were visibly overexposed, i.e. the 8-bit digital numbers (DN) of the background sky were 255 and parts any portion of the sky black (typically at 240-250 DN). Next, a method based on mathematical image morphology (Korhonen and Heikkinen, 2009) was applied to estimate the foliage and crown cover fractions. In this method, black-and-white canopy images are processed with morphological closing and opening operations that are well known in digital image processing (Gonzalez and Woods, 2002). As a result, a filter for "large" gaps was obtained. When a tuning parameter (called "structuring element" in image processing) was set so that "large" gaps only occurred between individual tree crowns (Korhonen and Heikkinen, 2009), the proportions of gaps inside and between individual crowns could be calculated.

2.3 Background signal retrieval method with Earth Observation data

The total reflectance of a pixel (R) results from the weighted linear combination of reflectance values by the forest canopy, forest background and their sunlit and shaded components (Li and Strahler, 1985; Chen et al., 2000; Bacour and Bréon, 2005; Chopping et al., 2008; Roujean et al., 1992):

$$R = k_T R_T + k_G R_G + k_{ZT} R_{ZT} + k_{ZG} R_{ZG} \quad (1)$$

which includes reflectivities of the sunlit crowns (R_T), sunlit understory (R_G), shaded crowns (R_{ZT},), and shaded understory (R_{ZG}). R_G marks the BRF of the target (understory). The k_j are the proportions of these components at the chosen view angle or in the instantaneous field of view of the sensor at given irradiation geometry. Following Canisius and Chen (2007), we derive the understory reflectivity (R_G) with the assumption that the reflectivities of overstory and understory at the given illumination geometry differ little between chosen view angles. While the components may not fully meet the definition of Lambertian reflectors (i.e. reflecting electromagnetic radiation equally in all directions), several previous studies (e.g. Bacour and Bréon, 2005; Deering et al., 1999; Peltoniemi et al., 2005) found forward-scattering reflectance factors of various targets

Table 2. Stand parameters for the Four-Scale model

Stand	Deciduous	Coniferous
Stand density (trees/ha)	500,1000,2000	500,1000,2000
Tree height (m)	25	16
Length of live crown (m)	9.2	4.2
Radius of crown projection (m)	1.87	1.5
Leaf area index (m^2/m^2)	1,2,3	1,2,3

off the principal plane to be fairly constant. The most suitable viewing configuration for the retrieval has been identified by Pisek et al. (2015a) using a high angular resolution BRF dataset of Kuusk et al. (2014) and accompanying *in situ* measurements of understory reflectance factors (Kuusk et al., 2013). The configuration consists of the BRF at nadir (R_n= 0 degrees) with solar zenith angle (SZA) corresponding to the Sun's position at 10:00 local time for given day and another zenith angle (R_a= 40 degrees) with relative azimuth angle PHI = 130 degrees. It can be expressed by the Eqs. (2), (3):

$$R_n = k_{Tn}R_T + k_{Gn}R_G + k_{ZTn}R_{ZT} + k_{ZGn}R_{ZG} \quad (2)$$
$$R_a = k_{Ta}R_T + k_{Ga}R_G + k_{ZTa}R_{ZT} + k_{ZGa}R_{ZG} \quad (3)$$

The proportions of the components (k_j) were obtained using the four-scale model (Chen and Leblanc, 1997) with parameters for generalized deciduous and coniferous tree stands as an input (see Table 2) (Kuusk et al., 2013). The understory reflectance at the desired wavelengths can be calculated by combining and solving equations (2) and (3) and insertion of R_n and R_a estimates derived from appropriate Earth Observation data. The individual components (sunlit/shaded overstory and understory) cannot be resolved with the MODIS spatial resolution. The reflectances of shaded tree crowns (R_{ZT}) and understory (R_{ZG}) are related to sunlit ones via M as R_{ZT} =M· R_T and R_{ZG}=M· R_G, where M=R_Z/R for a reference target, which can be measured in the field, or predetermined with the four-scale model. Here, the same M is assumed for overstory trees as well as understory. Based on his field work in Canadian boreal forests, White (1999) suggested that an angularly constant, wavelength dependent M values may be appropriate, at least during the growing season. The input stand parameters from Table 2 may not be always precisely known while retrieving the understory signal over larger areas. Figure 2 shows the relationships between the available *in situ* data for tree heights or tree densities over our study sites with the 1-km^2 resolution estimates from the global maps of Simard et al. (2011) and Crowther et al. (2015). The weak relationships indicate the current unsuitability of the site-specific variable estimates of interest (tree height, tree density) from currently available global maps at a given spatial resolution for our purpose. At the same time, the calculated mean values for the tree heights of needleleaved (17.5 m) and broadleaved tree stands (22.7 m) from Simard et al. (2011) over the study sites were reasonably close to our original generalized input parameter values in Table 2. Following Gemmell (2000), we opted to report a range of understory NDVI (NDVIu) values obtained with the combinations of parameter values from Table 2 for each site and date. Specifying the correct constraints

Figure 2. (A) Relationship between available *in situ* estimates of tree height (m) with Simard et al.'s, (2011) estimate; (B) relationship between available *in situ* estimates of tree density (trees/ha) with Crowther et al.'s (2015) estimates (DBF-deciduous broadleaf forest; EBF – evergreen broadleaf forest; DNF – deciduous needleleaf forest; ENF – evergreen needleleaf forest; MF – mixed forest).

(window) for background alone has been previously found to greatly reduce the errors in the estimation of overstory parameters (Gemmell, 2000).

2.4 MODIS BRDF data

The MCD43A1 V6 Bidirectional Reflectance Distribution Function and Albedo (BRDF/Albedo) model parameter dataset is a 500 meter gridded daily product. MCD43A1 is generated by inverting multi-date, multi-angular, cloud-free, atmospherically corrected, surface reflectance observations acquired by MODIS instruments on board the Terra and Aqua satellites over a 16-day period (Wang et al., 2018). The Julian date represents the 9th day of the 16-day retrieval period, and consequently the observations are further weighted to estimate the BRDF/Albedo for that particular day of interest. The MCD43A1 algorithm uses all high quality observations that adequately sample the viewing hemisphere to fit an appropriate semiempirical BRDF model (the RossThickLiSparse-reciprocal model, Roujean et al., 1992; Lucht et al., 2000) for that location and date of interest. We computed the bidirectional reflectance factor (BRF) at the top of canopy with the isotropic parameter and two (volumetric and geometric) kernel functions (Roujean et al., 1992) for MODIS band 1 (red, 620–670 nm) and band 2 (NIR, 841–876 nm). We used the Ross and Li kernels to reconstruct the bidirectional reflectance factor (BRF) values for required geometries (see section 2.3) for each date, and then derived the understory signal using the formulas described in Section 2.3. The associated data quality (MCD43A2) product was employed to assess the effect of retrieval quality on the accuracy of the calculated understory signal. All MODIS data have been accessed and processed through Google Earth Engine (Gorelick et al., 2017).

2.5 Spatial representativeness assessment of the validation sites

220 A method developed by Román et al. (2009), and refined by Wang et al. (2012, 2014, 2017) was adopted for evaluating the spatial representativeness of *in situ* measurements to assess the uncertainties arising from a direct comparison between field-measured forest understory spectra and the corresponding estimates with MODIS BRDF data. To characterize the spatial representativeness of a test site to represent a satellite retrieval, this method uses three variogram model parameters (the range, sill, and nugget), obtained by the analysis of near nadir surface reflectances from cloud free 30 m Landsat/Operational Land

225 Imager (OLI) data (Román et al., 2009) collected as close to the sampling date as possible. Where valid imagery was not available within a reasonable window of the sampling date, imagery from the corresponding season of a different year was used. As such, the analysis was done to illustrate the representativeness of the tower site with respect to a particular point in time.

230 Campagnolo et al. (2016) showed that the effective spatial resolution of 500 m gridded MODIS BRDF product at mid latitudes is around 833 m by 618 m because of the varied footprint of the source multi-angular surface reflectance observations. We analyzed each site with five different spatial extents (0.275 km, 0.5 km, 1 km, 1.5 km, 2 km) to assess and illustrate the changes in spatial representativeness with different spatial resolutions.

3 Results and Discussion

3.1 Spatial representativeness

235

Table 1 provides the assessment of spatial heterogeneity for all sites included in this study using OLI subsets acquired around the time of *in situ* measurements. The example results for the ICOS sites Norunda (SE-Nor) in Sweden and Wüstebach (DE-RuW) in Germany, using three OLI subsets, are shown in Figure 3. The variogram functions with relevant model parameters for the two sites are displayed in Figure 3B and D. The range corresponds to the value on the x-axis where the model flattens

240 out. There is no further correlation of a biophysical property associated with that point beyond the range value. The sill is the ordinate value of the range. Smaller sill value indicates a more homogenous surface (less variation in surface reflectance). Surface can be considered spatially representative with respect to the MODIS footprint when the sill value is < 5.0e-04 (Román et al., 2009; Wang et al., 2017). The sill values for all spatial extents are well below the value of 5.0e-04 up to 1 km spatial resolution in case of Norunda (Figure 3B), which indicates that the field measurements shall be representative and allow

245 comparison with MODIS retrievals at a 500 m spatial resolution. While the Wüstebach site can be considered spatially homogeneous within the immediate vicinity of 275 m around the tower, the sill value exceeds the criteria of 5.0e-04 at > 0.5 km spatial resolution. During late summer/early autumn of 2013, trees were almost completely removed in an area of 9 ha west of the tower in order to promote the natural regeneration of near-natural deciduous forest from spruce monoculture forest. The clear-felling area can be seen on Figure 3D. This action resulted in increasing the spatial heterogeneity
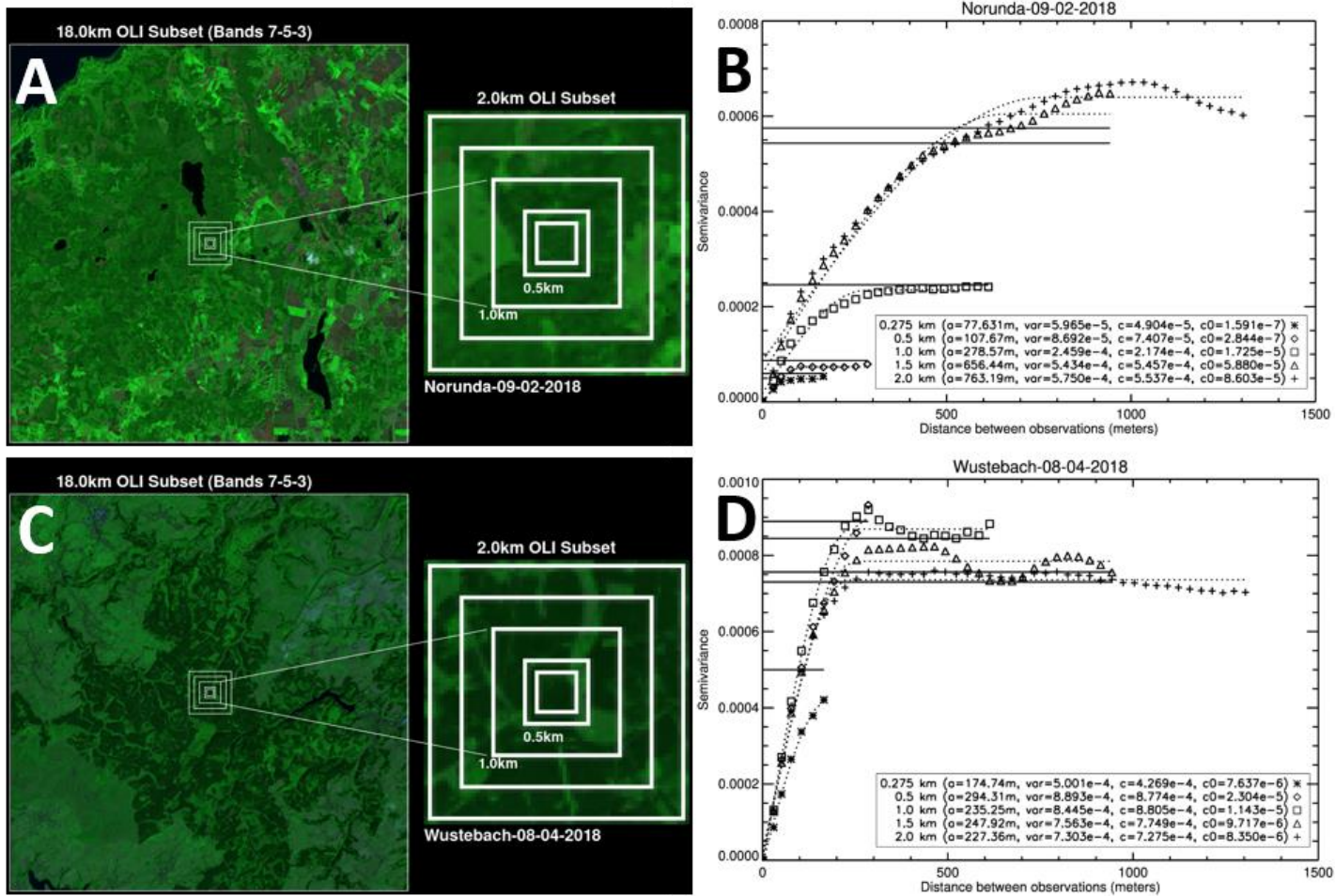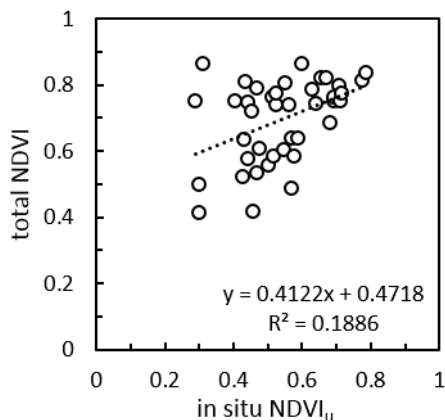
Figure 3. Shortwave BRF composites centered at ICOS sites (A) Norunda in Sweden and (C) Wüstebach in Germany. (B,D) Variogram estimators (points), spherical model results (dotted curves), and sample variances (solid straight lines) obtained over the sites with OLI subsets and spatial elements of 0.275 km, 0.5 km, 1.0 km, 1.5 km, and 2 km as a function of distance between observations. Variogram legend explanations: a - variogram range; var - sample variance; c - variogram sill; c0 = nugget variance.

of this ICOS site. *In situ* measurements collected within the footprint of the Wüstebach tower thus cannot be deemed fully comparable with the retrievals with MODIS at a 500 m spatial resolution. Overall most of the sites were found representative at the spatial resolution of MODIS BRDF gridded data. The non-representative cases and the effect on the understory signal retrieval and agreement with corresponding *in situ* measurements carried within the measurement footprint of the individual towers are further discussed in Sections 3.2 and 3.3. Román et al. (2009) provide further details on the assessment of spatial representativeness using a set of four geostatistical attributes derived from semivariograms.
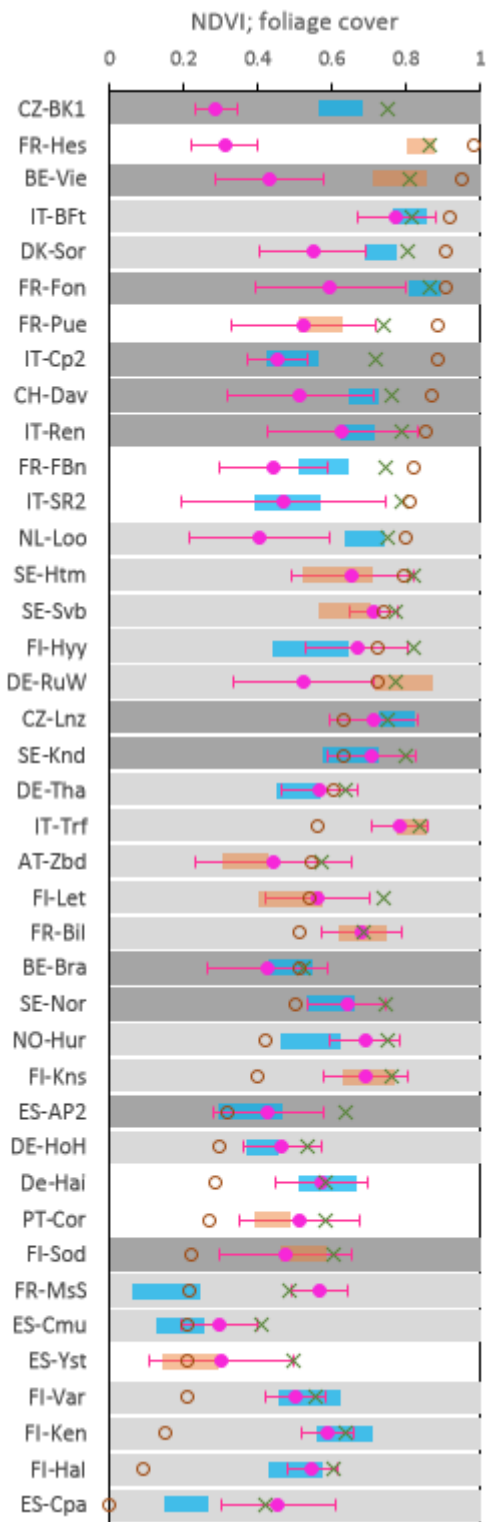
11

Figure 4. Relationship between total (overstory+understory) NDVI values computed from nadir NDVI values using MODIS BRDF/albedo data and *in situ* measured understory NDVI values over the study sites.

3.2 NDVI ranges

There is only a weak relationship between the total (overstory + understory) NDVI signal retrieved with MODIS BRDF data and corresponding *in situ* understory NDVI measurements (R^2=0.19; Figure 4). Total NDVI values alone do not allow one to disentangle the correct understory signal. In contrast, our retrieval method could track understory signal dynamics over a broad NDVI range (Figure 5). The predicted understory NDVI ranges were beyond the uncertainty limits of *in situ* understory measurements (corresponding to ± 1 standard deviation here) in less than 15% of cases. These sites with poor retrievals were carefully investigated to identify the issues precluding good results. Below we focus on a discussion of results where the predicted and *in situ* measured NDVI ranges of understory layer did not agree.

The understory dominated the overall signal of open shrubland at the Cortes de Pallas (ES-CPa) site and the deciduous broadleaf forest site at Montiers (FR-MsS) during the leaf-off part of the season (Figure 5). Both sites were found to be spatially representative for comparison with MODIS footprint data at the time of available *in situ* measurements (Table 1). There are only a very few trees scattered across the Cortes de Pallas site, and ground vegetation is fully exposed. Extremely low tree density does not match with any original generalized input parameter values in Table 2 and the predicted understory signal does not match well with *in situ* measurements. *In situ* measurements at Montiers were carried during leaf-off part of the season, which allowed full exposure of the understory. Despite this, the predicted understory NDVI range from the MODIS data did not overlap with the *in situ* measurements at Montiers at all. However, the MODIS BRDF values for these sites were marked with lower data quality flags (QA>1), which correctly signals a decrease in accuracy in the calculations of the understory reflectance as well. Overall, our results confirm that under conditions of very low tree density/leaves-off conditions, the understory signal can be assumed identical with the total scene NDVI.

NDVI; foliage cover

	0	0.2	0.4	0.6	0.8	1
CZ-BK1						
FR-Hes						
BE-Vie						
IT-BFt						
DK-Sor						
FR-Fon						
FR-Pue						
IT-Cp2						
CH-Dav						
IT-Ren						
FR-FBn						
IT-SR2						
NL-Loo						
SE-Htm						
SE-Svb						
FI-Hyy						
DE-RuW						
CZ-Lnz						
SE-Knd						
DE-Tha						
IT-Trf						
AT-Zbd						
FI-Let						
FR-Bil						
BE-Bra						
SE-Nor						
NO-Hur						
FI-Kns						
ES-AP2						
DE-HoH						
De-Hai						
PT-Cor						
FI-Sod						
FR-MsS						
ES-Cmu						
ES-Yst						
FI-Var						
FI-Ken						
FI-Hal						
ES-Cpa						

13

Figure 5. Estimated understory NDVI (NDVIu) ranges for selected days (see Section 2.3 how the ranges are obtained; blue bars for site representative retrievals; orange bars for possible non site representative retrievals), *in situ* measurements (mean +/- 1 standard deviation shown in purple), computed nadir total (understory+overstory) NDVI values from MODIS BRDF/albedo data (green crosses). Fraction of foliage cover shown with brown open circles. MODIS BRDF parameters with lower quality flags are indicated with light gray (QA=1) or dark gray (QA>1) bars. QA = 0 – best quality, full inversion; QA = 1 good quality, full inversion (including the cases with no clear sky observations over the day of interest and those with a Solar Zenith Angle > 70°); QA > 1 – lower quality magnitude inversion using archetypal BRDF shapes (for details please see Schaaf et al. (2002).

The performance of the method turns out to be limited over sites with a closed canopy such as Bílý Kříž (CZ-BK1), Hesse (FR-Hes), or Vielsalm (BE-Vie) (Figure 5). This is because shadowing effect makes diffuse scattering the dominant mechanism in such stands, and understory carries only a negligible influence on the top-of-canopy signal. Bosco Fontana (IT-BFt) is another broadleaf forest site with very high foliage cover (FC=0.91), yet the predicted understory NDVI range entirely overlaps with the collected *in situ* values. It should be noted that in contrast to other sites with closed canopies, Bosco Fontana has a very dense vegetation throughout the full vertical profile, and no clear distinction between overstory and understory can be made. Our results (Figure 5) indicate that in general reliable, independent retrieval of understory signal is not possible if foliage cover exceeds 85 %.

MODIS BRDF data were of the best quality in the case of Font Blanche site (FR-FBn). The canopy here was also relatively open (FC=0.18), yet the predicted understory NDVI range was higher than the lower NDVI captured by the *in situ* understory measurements. The Font Blanche site has a dense intermediate layer dominated by juvenile holm oaks (*Quercus ilex L.*) with a mean height of 6 m (Figure 7). Although the site was deemed spatially homogeneous at MODIS footprint scale (Table 2), the tall, dense layer made it impossible to obtain truly representative *in situ* measurements of understory reflectance. A similar situation with a tall shrub layer and thus a mismatch between the available *in situ* measurements and the predicted range of understory NDVI values was also encountered at another pine-dominated, spatially homogeneous site at Loobos (NL-Loo). Under such conditions the understory NDVI values retrieved with EO data might actually provide a more complete picture of understory condition.

MODIS BRDF data were also of the best quality over the Coruche (PT-Cor) site with a very open canopy (FC= 0.272). Such scenario should be optimal for the understory signal retrieval; yet the *in situ* measured NDVI of the understory is still higher than the predicted range with MODIS BRDF data. This disagreement appears to be caused by the presence of a water reservoir within the footprint of the MODIS pixel overlapping this site, which has contributed to lower reflectance in the red and NIR part of the spectrum. The water surface was not sampled during *in situ* measurements. Similar effect of nearby lake can be also observed in case of the Hurdal (NO-Hur) site.

As discussed in section 2.5, clear-felling was carried near the Wüstebach (DE-RuW) tower in 2013. Our assessment of site homogeneity showed that the site cannot be considered spatially homogeneous at the gridded 500 m spatial resolution of MODIS pixels (Figure 3D). The clear-felling action exposed the understory and encouraged the growth, resulting in an overlap of the total and retrieved understory signal by MODIS BRDF data. *In situ* measurements carried within the still forested part

of the site around the tower with greater canopy closure resulted in lower understory NDVI values. The Wüstebach site illustrates the importance of taking into account the spatial heterogeneity of a given site while comparing *in situ* measurements with EO observations at the corresponding scale. The proposed framework by Román et al. (2009) and Wang et al. (2017) using semivariograms is an efficient tool for evaluating site spatial representativeness.

330

In summary, while the understory retrieval algorithm was originally developed for conditions within the boreal region forests (Canisius and Chen, 2007), Figure 5 suggests encouraging performance of the retrieval algorithm over a much wider range of different forest sites. Reliable retrievals of forest understory appear to be feasible while taking into account the limitations due to site heterogeneity, foliage cover, and input data quality.

335 **3.3 Seasonal courses**

Figure 6 offers the overview of seasonal dynamics of understory for six select sites over the full latitudinal range (67°N - 38°N) across Europe.

The Station for Measuring Ecosystem-Atmosphere Relations in Värriö (Fi-Var) located in northern Finland (67°46'N, 340 29°35'E), represents a subarctic climate regime near the northern timberline. This site experiences very rapid increases in NDVI values at the beginning of the growing season (Figure 6A). This is linked with the disappearance of snow and exposure of the underlying understory vegetation, consisting predominantly of moss and lichen. The overstory coverage by Scots pine trees is sparse, and the overall NDVI signal fluctuations during the year are governed by understory layer. This site is also often covered with clouds, which prevents acquisition of large number of good quality MODIS observations. However, *in situ* 345 understory NDVI measurements fall within the predicted NDVI range when the MODIS data were acquired early in the growing season (DOY 165), even despite a lower quality of MODIS data (QA=1). No MODIS observations can be made of this site after DOY 259, due to insufficient amount of light.

The forest floor is mainly covered by moss at Norunda (SE-Nor) as well. While understory NDVI values reach similar values 350 in summer at both sites (Figure 6A-B), the snow disappears earlier at Norunda which results in earlier onset of higher understory NDVI values. *In situ* measurements fit very well within the predicted range with MODIS data on DOY 295. While Värriö has a higher tree density (748 trees/ha) than Norunda (600 trees/ha), Norunda, dominated with Norway spruce trees, has much higher foliage cover (FC=0.5 at Norunda compared to FC=0.21 at Värriö). The understory signal contribution is smaller and the total NDVI is higher at Norunda. The Norunda site provides yet another excellent demonstration of the 355 influence of MODIS data quality on the understory NDVI retrievals as well. There was a repeated unrealistic fluctuation of understory NDVI values with the period of DOY 229-260 (Figure 6B). The MODIS BRDF data during that period were marked with lower data quality flags (QA>1).
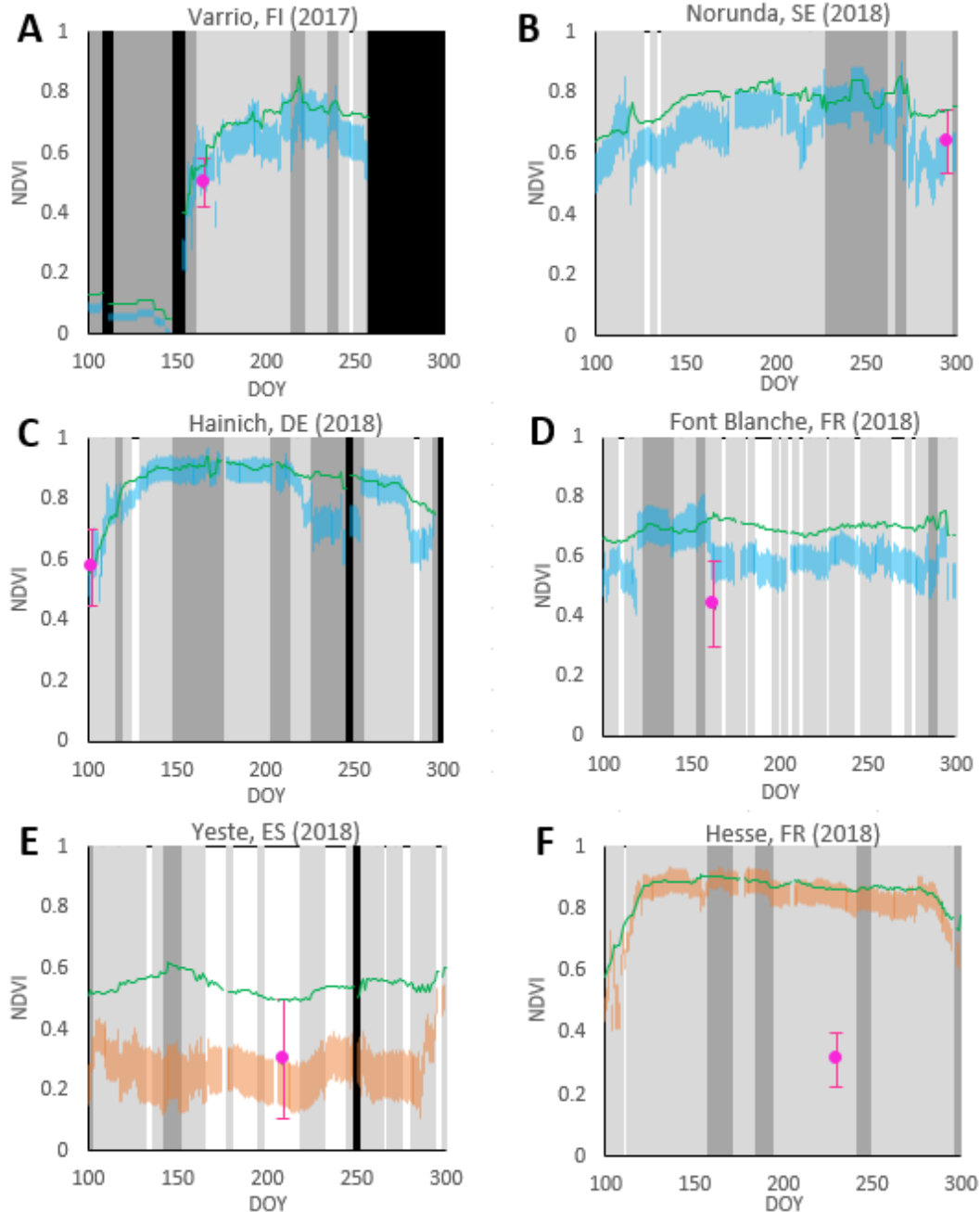
15

Figure 6. Seasonal courses of estimated understory NDVI (NDVIu) ranges (blue bars for site representative retrievals; orange bars for possible site non-representative retrievals), nadir total (understory+overstory) NDVI values from MODIS BRDF/albedo data (green lines), *in situ* measurements (mean +/- 1 standard deviation shown in purple) over select study sites. Gray bars mark MODIS BRDF parameters with lower quality flags (light gray, QA=1; dark gray, QA>1); black bars - no data available.

Figure 7. Foliage stratification between overstory and understory bushes at ICOS site Font Blanche in south-east France. Please note that the understory *in situ* measurements reported in Figure 6 did not include the tall (h>2 m) bushes located under the *Pinus halepensis* dominated overstory.

370

Very good agreement is observed among *in situ* measurements, understory and total NDVI signal from MODIS (Figure 6C) at Hainich (DE-Hai) at the beginning of the growing season (DOY=102). The site is dominated with deciduous beech trees, which were leafless when the *in situ* measurements were taken. This allowed a full exposure of the understory which dominated

375 the total reflectance signal from the stand during that moment in the season. The understory coverage was a mixture of litter and sprouting green understory. Later on, Hainich test site develops quickly an overstory layer with LAI values reaching up to 5 (Pinty et al., 2011). Such dense layer would prevent the retrieval of true understory signal with our methodology. This is confirmed by the unrealistic very close agreement between the very high NDVI values (NDVI ~ 0.9) obtained from the total and understory signal at Hainich test site during the peak of growing season (Figure 6C). However, this shortcoming would be

17

mitigated by the fact that in such cases the understory may be negligible in terms of LAI and overall contribution to the total signal.

Clear difference can be observed between the total and understory NDVI values at Font Blanche (FR-FBn) for most of the growing season (Figure 6D). The site is composed of an overstory top stratum (13 m) dominated by Aleppo pines (*Pinus halepensis Mill*), an intermediate stratum (6 m) dominated by holm oaks (*Quercus ilex L.*) and a shrub stratum (Simioni et al., 2020). Rainfall occurs mainly during autumn and winter with about 75% between September and April. The higher NDVIu values derived from the MODIS BRDF data during the period DOY 120-160 may be treated with caution due to the more frequent flagging of the MODIS inputs with lower data quality flags (Figure 6D). Even lower understory NDVI values (NDVIu range 0.15-0.35) occur at another site with a Mediterranean-type climate, Yeste in Spain (Figure 6E). The seasonal course of NDVI values here, with a low variation, is quite similar with Font Blanche. The increase in understory NDVI values in the autumn from DOY 288 is linked with the on-set of the rainfall period.

As illustrated above, given the high quality of MODIS BRDF data, the understory signal retrieval method performs well with forests with open canopy. However, it is not quite possible to separate understory signal in closed canopies. There is an obvious disagreement between available *in situ* measurements and the predicted understory NDVI range at Hesse (FR-Hes) (Figure 6F) which could be only partly explained by the insufficient spatial homogeneity of the site at the MODIS pixel footprint (Table 2). Hesse has a high foliage cover (FC = 0.98), LAI up to 7 and tall trees (h > 23 m). Understory would then have a negligible influence on the top-of-canopy signal. The visibility and contribution of understory signal also diminishes even further at off-nadir viewing directions (Rautiainen et al., 2008). Figure 6F confirms that in such situations the retrieval method cannot provide the correct, independent estimation of the understory signal. At the same time it should be noted that for closed canopies the understory signal (or lack of information about it) is not critical for the retrieval of biophysical properties of prime interest—LAI and fAPAR of the upper forest canopy layer with remote sensing (Garrigues et al., 2008; Weiss et al., 2014).

4 Conclusions

We report on the performance of a physically based approach to estimate understory NDVI from daily MODIS BRDF/albedo data, at a 500 m gridded spatial resolution, over the extended network of the Integrated Carbon Observing System (ICOS) forest ecosystem sites, distributed along wide latitudinal and elevational ranges (68°N - 38°N, 12-1864 m a.s.l.) across Europe. The analysis corresponds to a Stage 1 validation as defined by the CEOS (Nightingale et al., 2011; Weiss et al., 2014). The method can deliver reasonable retrievals over different forest types with canopies where foliage cover does not exceed 85 %. The performance of the method was found limited over forests with closed canopies (high foliage cover), where the signal from understory gets much attenuated. Our results illustrate the importance of considering both the spatial heterogeneity of the field site, as well as limitations and documented quality of the MODIS BRDF product. The results from the *in situ*

measurements of understory layer can be valuable, in themselves, as source of information over the wide array of forest understory conditions contained within the tower footprints of individual ICOS forest ecosystem sites and serve as an input for improved modelling of local carbon and energy fluxes.

415

425

References

Bacour, C., and Bréon, F.M.: Variability of biome reflectance directional signatures as seen by POLDER. Remote Sensing of

435 Environment, 98, 80–95, 2005.

Baret, F., Morisette, J. T., Fernandes, R. A., Champeaux, J. L., Myneni, R. B., Chen, J., et al.: Evaluation of the representativeness of networks of sites for the global validation and intercomparison of land biophysical products: Proposition of the CEOSBELMANIP. IEEE Transactions on Geoscience and Remote Sensing, 44, 1794−1803, 2006.

Campagnolo, M.L., Sun, Q., Liu, Y., Schaaf, C., Wang, Z., Román, M.O.: Estimating the effective spatial resolution of the

440 operational BRDF, albedo, andnadir reflectance products from MODIS and VIIRS. Remote Sens. Environ. 175,52–64, http://dx.doi.org/10.1016/j.rse.2015.12.033, 2016.

Canisius, F., and Chen, J.M.: Retrieving forest background reflectance in a boreal region from Multi-angle Imaging SpectroRadiometer (MISR) data. Remote Sensing of Environment, 107, 312–321, 2007.

Chen, J.M., Li, X., Nilson, T., Strahler, A.: Recent advances in geometrical optical modeling and its applications. Remote Sensing Reviews, 18, 227–262, 2000.

Chopping, M., Moisen, G.G., Su, L.H., Laliberte, A., Rango, A., Martonchik, J.V., et al.: Large area mapping of southwestern crown cover, canopy height, and biomass using the NASA Multiangle Imaging Spectro-Radiometer. Remote Sensing of Environment, 112, 2051–2063, 2008.

Clark, D. A., Brown, S., Kicklighter, D. W., Chambers, J. Q., Thomlinson, J. R., Ni, J.: Measuring net primary production in forests: concepts and field methods. Ecological Applications, 11(2), 356-370, 2001.

Crowther, T. W., et al.: Mapping tree density at a global scale, Nature, 525, 201–205, 2015.

Deering, D.W., Eck, T.F., and Banerjee, B.: Characterization of the reflectance anisotropy of three boreal forest canopies in spring–summer. Remote Sens. Environ., 67, 205–229, 1999.

Garrigues, S., et al.: Validation and intercomparison of global leaf area index products derived from remote sensing data, J. Geophys. Res., 113, G02028, doi:10.1029/2007JG000635, 2008.

Gemmell, F.: Testing the utility of multi-angle spectral data for reducing the effects of background spectral variations in forest reflectance model inversion, Remote Sens. Environ., 72, 46–63, 2000.

Gielen, B., de Beeck, M.O., Loustau, D., Ceulemans, R., Jordan, A. and Papale, D.: Integrated Carbon Observation System (ICOS): An Infrastructure to Monitor the European Greenhouse Gas Balance, In Terrestrial Ecosystem Research Infrastructures: Challenges and Opportunities. , pp. 505-520. CRC press, 2017.

Gonzalez, R.C., Woods, R.E.: Digital Image Processing. 2nd ed. Prentice Hall, Upper Saddle River (NJ). 793 p., 2002.

Gorelick, N., Hancher, M., Dixon, M., Ilyushchenko, S., Thau, D., Moore, R.: Google earth engine: planetary-scale geospatial analysis for everyone. Remote Sens. Environ. 202, 18–27, 2017.

Gschwantner, T., Schadauer, K., Vidal, C., Lanz, A., Tomppo, E., di Cosmo, L., Robert, N., Englert Duursma, D. & Lawrence, M.: Common tree definitions for national forest inventories in Europe. Silva Fennica 43(2): 303–321, 2009.

Jiao, T., Liu, R., Liu, Y., Pisek, J., Chen, J. M.: Mapping global seasonal forest background reflectivity with Multi-angle Imaging Spectroradiometer data. Journal of Geophysical Research: Biogeosciences, 119(6), 1063-1077, 2014.

Kim, D., Oren, R., and Qian, S. S.: Response to CO2 enrichment of understory vegetation in the shade of forests, Glob. Change Biol., 22, 944–956, doi:10.1111/gcb.13126, 2016.

Korhonen, L., Heikkinen, J.: Automated analysis of in situ canopy images for the estimation of forest canopy cover. For Sci 55:323–334, 2009.

Kuusk, A., Lang, M., Kuusk, J.: Database of optical and structural data for the validation of forest radiative transfer models. In A.A. Kokhanovsky (Ed.), Radiative transfer and optical properties of atmosphere and underlying surface. Light Scattering Reviews, 7. (pp. 109–148). Berlin, Germany: Springer, 2013.

Kuusk, A., Kuusk, J., Lang, M.: Measured spectral bidirectional reflection properties of three mature hemiboreal forests. Agricultural and Forest Meteorology, 185, 14–19, 2014.

Law, B. E., Van Tuyl, S., Cescatti, A., Baldocchi, D. D.: Estimation of leaf area index in open-canopy ponderosa pine forests at different successional stages and management regimes in Oregon. Agricultural and Forest Meteorology, 108(1), 1-14, 2001.

Li, X., and Strahler, A.: Geometric-optical modelling of a conifer forest canopy. IEEE Transactions on Geoscience and Remote Sensing, 23, 207–221, 1985.

Luyssaert, S., Inglima, I., Jung, M., Richardson, A. D., Reichstein, M., Papale, D., et al.: CO2 balance of boreal, temperate, and tropical forests derived from a global database. Global Change Biology, 13(12), 2509-2537, 2007.

Macfarlane, C., Hoffman, M., Eamus, D., Kerp, N., Higginson, S., McMurtrie, R., Adams, M.: Estimation of leaf area index in eucalypt forest using digital photography. Agricultural and Forest Meteorology 143 (3–4), 176–188, 2007.

Marques, M. C. M. and Oliveira, P. E. A. M.: Phenology of canopy and understory species of two Coastal Plain Forests in Southern Brazil, Brazilian J. Bot., 27, 713–723, doi:10.1590/s0100-84042004000400011, 2004.

McDonald, A. J., Gemmell, F. M., and Lewis, P. E.: Investigation of the utility of spectral vegetation indices for determining information on coniferous forests. Remote Sens. Environ. 66:250–272, 1998.

Miller, J., et al.: Seasonal change in the understory reflectance of boreal forests and influence on canopy vegetation indices, J. Geophys. Res., 102(D24), 29,475–29,482, doi:10.1029/97JD02558, 1997.

Nightingale, J., Schaepman-Strub, G., Nickeson, J., Leads, L.F.A.: Assessing satellite-derived land product quality for earth system science applications: overview of the CEOS LPV sub-group. In: Proceedings of the 34th International Symposium on Remote Sensing of Environment. Sydney, NSW, Australia, 10–15 April 2011.

Nobis, M., and Hunziker, U.: Automatic thresholding for hemispherical canopy-photographs based on edge detection. Agricultural and Forest Meteorology, 128(3-4), 243-250. https://doi.org/10.1016/j.agrformet.2004.10.002, 2005.

Pinty, B., Jung, M., Kaminski, T., Lavergne, T., Mund, M., Plummer, S., Thomas, E., Widlowski, J. -L.: Evaluation of the JRC-TIP 0.01° products over a mid-latitude deciduous forest site, Remote Sensing of Environment, 115, 3567-3581, 2011.

Peltoniemi, J., Kaasalainen, S., Näränen, J., Rautiainen, M., Stenberg, P., Smolander, H., et al.: BRDF measurement of understory vegetation in pine forests: Dwarf shrubs, lichen and moss. Remote Sensing of Environment, 94, 343–354, 2005.

Pisek, J., and Chen, J.M.: Mapping forest background reflectivity over North America with multi-angle imaging spectroradiometer (MISR) data. Remote Sensing of Environment, 113, 2412–2423, 2009.

Pisek, J., Chen, J.M., Miller, J.R., Freemantle, J.R., Peltoniemi, J.I., Simic, A.: Mapping forest background reflectance in a boreal region using multi-angle Compact Airborne Spectrographic Imager (CASI) data. IEEE Transactions on Geoscience and Remote Sensing, 48, 499–510, 2010.

Pisek, J., Rautiainen, M., Heiskanen, J., Mõttus, M.: Retrieval of seasonal dynamics of forest understory reflectance in a Northern European boreal forest from MODIS BRDF data. Remote Sensing of Environment, 117, 464–468, 2012.

Pisek, J., Lang, M., Kuusk, J.: A note on suitable viewing configuration for retrieval of forest understory reflectance from multi-angle remote sensing data, Remote Sens. Environ., 156, 242–246, 2015a.

Pisek, J., Rautiainen, M., Nikopensius, M., Raabe K.: Estimation of seasonal dynamics of understory NDVI in northern forests using MODIS BRDF data: Semi-empirical versus physically-based approach, Remote Sens. Environ., 163, 42–47, 2015b.

Pisek, J., Chen, J. M., Kobayashi, H., Rautiainen, M., Schaepman, M. E., Karnieli, A. et al.: Retrieval of seasonal dynamics of forest understory reflectance from semiarid to boreal forests using MODIS BRDF data. Journal of Geophysical Research: Biogeosciences, 121(3), 855-863, 2016.

Rautiainen, M., Lang, M., Mõttus, M., Kuusk, A., Nilson, T., Kuusk, J., Lükk, T.: Multi-angular reflectance properties of a hemiboreal forest: an analysis using CHRIS PROBA data. Remote Sensing of Environment, 112 (5), 2627−2642, 2008.

Rautiainen, M., Mõttus, M., Heiskanen, J., Akujärvi, A., Majasalmi, T., Stenberg, P.: Seasonal reflectance dynamics of common understory types in a northern European boreal forest. Remote Sensing of Environment, 115(12), 3020-3028, 2011.

Rentch, J. S., Fajvan, M. A., and Hicks, R. R.: Oak establishment and canopy accession strategies in five old-growth stands in the central hardwood forest region, Forest Ecol. Manage., 184, 285–297, doi:10.1016/s0378-1127(03)00155-5, 2003.

Román, M.O., Schaaf, C.B., Woodcock, C.E., Strahler, A.H., Yang, X., Braswell, R.H.,Curtis, P.S., Davis, K.J., Dragoni, D., Goulden, M.L.: The MODIS (CollectionV005) BRDF/albedo product: assessment of spatial representativeness overforested landscapes. Remote Sens. Environ. 113, 2476–2498, http://dx.doi.org/10.1016/j.rse.2009.07.009, 2009.

Roujean, J. -L., M. Leroy, and Deschamps, P. Y.: A bi-directional reflectance model of the Earth's surface for the correction of remote sensing data, J. Geophys. Res., 97(D18), 20,455–20,468, doi:10.1029/92JD01411, 1992.

Rouse, W. J., Haas Jr., H.R., Schell, A.J., Deering, W.D.: Monitoring vegetation systems in the Great Plains with ERTS, in Third ERTS Symposium, NASASP-351, vol. I, pp. 309–317, NASA, Washington, D. C., 1973.

Schaaf, C. B., Gao, F., Strahler, A. H., Lucht, W., Li, X., Tsang, T.: First operational BRDF albedo, nadir reflectance products from MODIS. Remote Sensing of Environment, 83, 135–148, 2002.

Schaepman, M. E., S. L. Ustin, A. J. Plaza, T. H. Painter, J. Verrelst, S. Liang: Earth system science related imaging spectroscopy-An assessment, Remote Sens. Environ., 113, S123–S137, 2009.

Schaepman-Strub, G., Schaepman, M. E., Painter, T. H., Dangel, S., Martonchik, J. V.: Reflectance quantities in optical remote sensing—Definitions and case studies. Remote Sensing of Environment, 103(1), 27-42, 2006.

Simard, M., Pinto, N., Fisher, J.B., Baccini, A.: Mapping forest canopy height globally with spaceborne lidar, J. Geophys. Res., 116, G04021, doi:10.1029/2011JG001708, 2011.

Simioni, G., Marie, G., Davi, H., Martin-St Paul, N., Huc, R.: Natural forest dynamics have more influence than climate change on the net ecosystem production of a mixed Mediterranean forest. Ecol Model 416:108921, 2020.

Vogel, J. G. and Gower, S. T.: Carbon and nitrogen dynamics of boreal jack pine stands with and without a green alder understory, Ecosystems, 1, 386–400, doi:10.1007/s100219900032, 1998.

Tucker, C. J.: Red and photographic infrared linear combinations for monitoring vegetation. Remote Sens. Environ. 8, 127−150, 1979.

Wang, Z., Schaaf, C.B., Sun, Q., Kim, J., Erb, A.M., Gao, F., Román, M.O., Yang, Y., Petroy, S., Taylor, J.R.: Monitoring land surface albedo and vegetation dynamics using high spatial and temporal resolution synthetic time series from Landsat and the MODIS BRDF/NBAR/albedo product. Int. J. Appl. Earth Obs. Geoinf. 59, 104–117, 2017.

Wang, Z., Schaaf, C. B., Sun, Q., Shuai, Y., & Román, M. O. Capturing Rapid Land Surface Dynamics with Collection V006

545   MODIS BRDF/NBAR/Albedo (MCD43) Products. Remote Sensing of Environment, 207, 50–64, 2018.

Weiss, M., et al.: On line validation exercise (OLIVE): A web based service for the validation of medium resolution land products. Application to FAPAR products, Remote Sens., 6, 4190–4216, 2014.

White, H.P.: Investigations of boreal forest bidirectional reflectance factor (BRF), PhD. thesis, York University, Toronto, Ontario, Canada, 328 p., 1999.

550   White, P.H., Miller, J.R., Chen, J.M.: Four-scale linear model for anisotropic reflectance (FLAIR) for plant canopies—Part I: Model description and partial validation. IEEE Transactions on Geoscience and Remote Sensing, 39, 1073–1083, 2001.

White, H.P., Miller, J.R., Chen, J.M.: Four-scale linear model for anisotropic reflectance (FLAIR) for plant canopies—Part II: Validation and inversion with CASI, POLDER, and PARABOLA data at BOREAS. IEEE Transactions on Geoscience and Remote Sensing, 40, 1038–1046, 2002.

555